Encapsulation of a Concanavalin A/dendrimer glucose sensing assay within microporated poly (ethylene glycol) microspheres

Brian M. Cummins,[1,]* Jongdoo Lim,[2] Eric E. Simanek,[2] Michael V. Pishko,[3] and Gerard L. Coté[1]

[1]*Department of Biomedical Engineering, Texas A&M University,3120 TAMU, College Station, TX 77843–3120, USA*
[2]*Department of Chemistry, Texas A&M University, College Station, TX 77843, USA; present address, Department of Chemistry, Texas Christian University, Fort Worth, TX 76129, USA*
[3]*Department of Chemical Engineering, Texas A&M University, College Station, TX 77843, USA*
*brian.cummins@tamu.edu

Abstract: Proper management of diabetes requires the frequent measurement of a patient's blood glucose level. To create a long-term, minimally-invasive sensor that is sensitive to physiological concentrations of glucose a fluorescent glucose sensing assay using a competitive binding approach between fluorescently tagged Concanavalin-A (Con-A) and glycodendrimer is being developed. Until now, the essential step of effectively encapsulating this aggregative sensing assay while allowing a reversible response has yet to be reported. In this paper, a microporation technique is described in which microspheres are synthesized in a manner that creates fluid-filled pores within a poly (ethylene glycol) hydrogel. This dual-nature technique creates hydrophilic, biocompatible microcapsules in which the aggregative binding kinetics of the sensing assay within the pores are not constrained by spatial fixation in the hydrogel matrix. Confocal images displaying the localization of pockets filled with the assay within the polymeric matrix are presented in this paper. In addition, fluorescent responses to varying glucose concentrations, leaching studies, and long-term functionality of the encapsulated assay are demonstrated. To our knowledge, this is the first time that the Con-A/glycodendrimer assay has been shown to be reversible and repeatable within hydrogel spheres, including the display of functionality up to fourteen days under ambient conditions.

References and links

1. The Diabetes Control and Complications Trial Research Group, "The effect of intensive treatment of diabetes on the development and progression of long-term complications in insulin-dependent diabetes mellitus," N. Engl. J. Med. **329**(14), 977–986 (1993).
2. D. M. Nathan, P. A. Cleary, J. Y. Backlund, S. M. Genuth, J. M. Lachin, T. J. Orchard, P. Raskin, and B. Zinman; Diabetes Control and Complications Trial/Epidemiology of Diabetes Interventions and Complications (DCCT/EDIC) Study Research Group, "Intensive diabetes treatment and cardiovascular disease in patients with type 1 diabetes," N. Engl. J. Med. **353**(25), 2643–2653 (2005).
3. American Diabetes Association, "Economic costs of diabetes in the U.S. In 2007," Diabetes Care **31**(3), 596–615 (2008).
4. American Diabetes Association, "Standards of medical care in diabetes--2009," Diabetes Care **32**(Suppl 1), S13–S61 (2009).
5. C. L. Rohlfing, R. R. Little, H. M. Wiedmeyer, J. D. England, R. Madsen, M. I. Harris, K. M. Flegal, M. S. Eberhardt, and D. E. Goldstein, "Use of GHb (HbA1c) in screening for undiagnosed diabetes in the U.S. population," Diabetes Care **23**(2), 187–191 (2000).

6. J. Pickup, "Diabetic control and its measurements," *Textbook of Diabetes, third ed.*, 34.1–34.17, Blackwell (2003).
7. I. B. Hirsch, D. Armstrong, R. M. Bergenstal, B. Buckingham, B. P. Childs, W. L. Clarke, A. Peters, and H. Wolpert, "Clinical application of emerging sensor technologies in diabetes management: consensus guidelines for continuous glucose monitoring (CGM)," Diabetes Technol. Ther. **10**(4), 232–246 (2008).
8. R. J. McNichols and G. L. Coté, "Optical glucose sensing in biological fluids: an overview," J. Biomed. Opt. **5**(1), 5–16 (2000).
9. J. Wang, "Glucose biosensors: 40 Years of advances and challenges," Electroanalysis **13**(12), 983–988 (2001).
10. N. S. Oliver, C. Toumazou, A. E. Cass, and D. G. Johnston, "Glucose sensors: a review of current and emerging technology," Diabet. Med. **26**(3), 197–210 (2009).
11. J. Lambert, J. Morookian, S. Sirk, and M. Borchert, "Measurement of aqueous glucose in a model anterior chamber using Raman spectroscopy," J. Raman Spectrosc. **33**(7), 524–529 (2002).
12. A. M. Enejder, T. G. Scecina, J. Oh, M. Hunter, W. C. Shih, S. Sasic, G. L. Horowitz, and M. S. Feld, "Raman spectroscopy for noninvasive glucose measurements," J. Biomed. Opt. **10**(3), 031114 (2005).
13. D. Qi and A. J. Berger, "Chemical concentration measurement in blood serum and urine samples using liquid-core optical fiber Raman spectroscopy," Appl. Opt. **46**(10), 1726–1734 (2007).
14. I. Barman, C. R. Kong, N. C. Dingari, R. R. Dasari, and M. S. Feld, "Development of robust calibration models using support vector machines for spectroscopic monitoring of blood glucose," Anal. Chem. **82**(23), 9719–9726 (2010).
15. R. O. Esenaliev, K. V. Larin, I. V. Larina, and M. Motamedi, "Noninvasive monitoring of glucose concentration with optical coherence tomography," Opt. Lett. **26**(13), 992–994 (2001).
16. V. V. Sapozhnikova, D. Prough, R. V. Kuranov, I. Cicenaite, and R. O. Esenaliev, "Influence of osmolytes on in vivo glucose monitoring using optical coherence tomography," Exp. Biol. Med. (Maywood) **231**(8), 1323–1332 (2006).
17. H. A. MacKenzie, H. S. Ashton, Y. C. Shen, J. Lindberg, P. Rae, K. M. Quan, and S. Spiers, "Blood glucose measurements by photoacoustics," in *Biomedical Optical Spectroscopy and Diagnostics/Therapeutic Laser Applications*, E. Sevick-Muraca and J. Izatt, eds., Vol. 22 of OSA Trends in Optics and Photonics (Optical Society of America, 1998), paper BTuC1.
18. R. Weiss, Y. Yegorchikov, A. Shusterman, and I. Raz, "Noninvasive continuous glucose monitoring using photoacoustic technology-results from the first 62 subjects," Diabetes Technol. Ther. **9**(1), 68–74 (2007).
19. L. Zeng, G. Liu, D. Yang, Z. Ren, and Z. Huang, "Design of a portable noninvasive photoacoustic glucose monitoring system integrated laser diode excitation with annular array detection," Proc. SPIE **7280**, 72802F (2009).
20. R. R. Ansari, S. Böckle, and L. Rovati, "New optical scheme for a polarimetric-based glucose sensor," J. Biomed. Opt. **9**(1), 103–115 (2004).
21. Q. Wan, G. L. Coté, and J. B. Dixon, "Dual-wavelength polarimetry for monitoring glucose in the presence of varying birefringence," J. Biomed. Opt. **10**(2), 024029 (2005).
22. B. Malik and G. Coté, "Real-time dual wavelength polarimetry for glucose sensing," Proc. SPIE **7186**, 718604 (2009).
23. B. D. Cameron, J. S. Baba, and G. L. Coté, "Measurement of the glucose transport time delay between the blood and aqueous humor of the eye for the eventual development of a noninvasive glucose sensor," Diabetes Technol. Ther. **3**(2), 201–207 (2001).
24. B. D. Cameron and H. Anumula, "Development of a real-time corneal birefringence compensated glucose sensing polarimeter," Diabetes Technol. Ther. **8**(2), 156–164 (2006).
25. J. J. Burmeister, M. A. Arnold, and G. W. Small, "Noninvasive blood glucose measurements by near-infrared transmission spectroscopy across human tongues," Diabetes Technol. Ther. **2**(1), 5–16 (2000).
26. C. Vrančić, A. Fomichova, N. Gretz, C. Herrmann, S. Neudecker, A. Pucci, and W. Petrich, "Continuous glucose monitoring by means of mid-infrared transmission laser spectroscopy in vitro," Analyst (Lond.) **136**(6), 1192–1198 (2011).
27. L. Tolosa, H. Malak, G. Raob, and J. Lakowicz, "Optical assay for glucose based on the luminescence decay time of the long wavelength dye Cy5," Sens. Actuators B Chem. **45**(2), 93–99 (1997).
28. R. J. Russell, M. V. Pishko, C. C. Gefrides, M. J. McShane, and G. L. Coté, "A fluorescence-based glucose biosensor using concanavalin A and dextran encapsulated in a poly(ethylene glycol) hydrogel," Anal. Chem. **71**(15), 3126–3132 (1999).
29. S. D'Auria, N. Di Cesare, Z. Gryczynski, I. Gryczynski, M. Rossi, and J. R. Lakowicz, "A thermophilic apoglucose dehydrogenase as nonconsuming glucose sensor," Biochem. Biophys. Res. Commun. **274**(3), 727–731 (2000).
30. M. J. McShane, "Potential for glucose monitoring with nanoengineered fluorescent biosensors," Diabetes Technol. Ther. **4**(4), 533–538 (2002).
31. R. Ballerstadt, A. Polak, A. Beuhler, and J. Frye, "In vitro long-term performance study of a near-infrared fluorescence affinity sensor for glucose monitoring," Biosens. Bioelectron. **19**(8), 905–914 (2004).
32. J. Siegrist, T. Kazarian, C. Ensor, S. Joel, M. Madou, P. Wang, and S. Daunert, "Continuous glucose sensor using novel genetically engineered binding polypeptides towards in vivo applications," Sens. Actuators B Chem. **149**(1), 51–58 (2010).

33. B. L. Ibey, H. T. Beier, R. M. Rounds, G. L. Coté, V. K. Yadavalli, and M. V. Pishko, "Competitive binding assay for glucose based on glycodendrimer-fluorophore conjugates," Anal. Chem. **77**(21), 7039–7046 (2005).
34. C. Huet, M. Lonchampt, M. Huet, and A. Bernadac, "Temperature effects on the concanavalin A molecule and on concanavalin A binding," Biochim. Biophys. Acta **365**(1), 28–39 (1974).
35. H. Bittiger and H. Schnebli, *Concanavalin A as a Tool*, John Wiley & Sons, (1976).
36. J. S. Schultz, S. Mansouri, and I. J. Goldstein, "Affinity sensor: a new technique for developing implantable sensors for glucose and other metabolites," Diabetes Care **5**(3), 245–253 (1982).
37. S. Mansouri and J. Schultz, "Optical glucose sensor based on reversible competitive binding," IEEE, 112–115 (1984).
38. R. Ballerstadt and J. S. Schultz, "A fluorescence affinity hollow fiber sensor for continuous transdermal glucose monitoring," Anal. Chem. **72**(17), 4185–4192 (2000).
39. R. Ballerstadt, C. Evans, R. McNichols, and A. Gowda, "Concanavalin A for in vivo glucose sensing: a biotoxicity review," Biosens. Bioelectron. **22**(2), 275–284 (2006).
40. C. Kojima, K. Kono, K. Maruyama, and T. Takagishi, "Synthesis of polyamidoamine dendrimers having poly(ethylene glycol) grafts and their ability to encapsulate anticancer drugs," Bioconjug. Chem. **11**(6), 910–917 (2000).
41. D. A. Tomalia, L. A. Reyna, and S. Svenson, "Dendrimers as multi-purpose nanodevices for oncology drug delivery and diagnostic imaging," Biochem. Soc. Trans. **35**(1), 61–67 (2007).
42. M. Liu, K. Kono, and J. M. Fréchet, "Water-soluble dendritic unimolecular micelles: their potential as drug delivery agents," J. Control. Release **65**(1-2), 121–131 (2000).
43. M. T. Morgan, M. A. Carnahan, C. E. Immoos, A. A. Ribeiro, S. Finkelstein, S. J. Lee, and M. W. Grinstaff, "Dendritic molecular capsules for hydrophobic compounds," J. Am. Chem. Soc. **125**(50), 15485–15489 (2003).
44. H. T. Chen, M. F. Neerman, A. R. Parrish, and E. E. Simanek, "Cytotoxicity, hemolysis, and acute in vivo toxicity of dendrimers based on melamine, candidate vehicles for drug delivery," J. Am. Chem. Soc. **126**(32), 10044–10048 (2004).
45. M. F. Neerman, W. Zhang, A. R. Parrish, and E. E. Simanek, "In vitro and in vivo evaluation of a melamine dendrimer as a vehicle for drug delivery," Int. J. Pharm. **281**(1-2), 129–132 (2004).
46. E. R. Gillies and J. M. Fréchet, "Dendrimers and dendritic polymers in drug delivery," Drug Discov. Today **10**(1), 35–43 (2005).
47. A. J. Velazquez, M. A. Carnahan, J. Kristinsson, S. Stinnett, M. W. Grinstaff, and T. Kim, "New dendritic adhesives for sutureless ophthalmic surgical procedures: in vitro studies of corneal laceration repair," Arch. Ophthalmol. **122**(6), 867–870 (2004).
48. M. W. Grinstaff, "Biodendrimers: new polymeric biomaterials for tissue engineering," Chemistry **8**(13), 2838–2846 (2002).
49. P. Wu, X. Chen, N. Hu, U. C. Tam, O. Blixt, A. Zettl, and C. R. Bertozzi, "Biocompatible carbon nanotubes generated by functionalization with glycodendrimers," Angew. Chem. Int. Ed. Engl. **47**(27), 5022–5025 (2008).
50. W. Turnbull and J. Stoddart, "Design and synthesis of glycodendrimer," Rev. Mol. Biotechnol. **90**(3–4), 231–255 (2002).
51. C. C. Lee, J. A. MacKay, J. M. Fréchet, and F. C. Szoka, "Designing dendrimers for biological applications," Nat. Biotechnol. **23**(12), 1517–1526 (2005).
52. U. Gupta, H. B. Agashe, A. Asthana, and N. K. Jain, "Dendrimers: novel polymeric nanoarchitectures for solubility enhancement," Biomacromolecules **7**(3), 649–658 (2006).
53. B. Ibey, H. Beier, R. Rounds, M. Pishko, and G. Coté, "Dendrimer based fluorescent glucose sensor for diabetic monitoring," *Progress in Biomedical Optics and Imaging - Proceedings of SPIE,* (2006).
54. S. Cohen, T. Yoshioka, M. Lucarelli, L. H. Hwang, and R. Langer, "Controlled delivery systems for proteins based on poly(lactic/glycolic acid) microspheres," Pharm. Res. **08**(6), 713–720 (1991).
55. W. R. Gombotz and S. Wee, "Protein release from alginate matrices," Adv. Drug Deliv. Rev. **31**(3), 267–285 (1998).
56. S. Freiberg and X. X. Zhu, "Polymer microspheres for controlled drug release," Int. J. Pharm. **282**(1-2), 1–18 (2004).
57. A. A. Antipov and G. B. Sukhorukov, "Polyelectrolyte multilayer capsules as vehicles with tunable permeability," Adv. Colloid Interface Sci. **111**(1-2), 49–61 (2004).
58. C. S. Peyratout and L. Dähne, "Tailor-made polyelectrolyte microcapsules: from multilayers to smart containers," Angew. Chem. Int. Ed. Engl. **43**(29), 3762–3783 (2004).
59. Y. Zhu, J. Shi, W. Shen, X. Dong, J. Feng, M. Ruan, and Y. Li, "Stimuli-responsive controlled drug release from a hollow mesoporous silica sphere/polyelectrolyte multilayer core-shell structure," Angew. Chem. Int. Ed. Engl. **44**(32), 5083–5087 (2005).
60. M. McShane and Y. Lvov, "Layer-by-Layer Electrostatic Self-Assembly," in *Dekker Encyclopedia of Nanoscience and Nanotechnology,* Second Edition, ed. J. Schwarz, C. Contescu, K. Putyera, Eds.; Taylor & Francis, 1823–1840, (2009).
61. O. Kreft, A. M. Javier, G. B. Sukhorukov, and W. J. Parak, "Polymer microcapsules as mobile local pH-sensors," J. Mater. Chem. **17**(42), 4471–4476 (2007).
62. C. Gao, S. Moya, E. Donath, and H. Möhwald, "Melamine formaldehyde core decomposition as the key step controlling capsule integrity: optimizing the polyelectrolyte capsule fabrication," Macromol. Chem. Phys. **203**(7), 953–960 (2002).

63. D. V. Volodkin, N. I. Larionova, and G. B. Sukhorukov, "Protein encapsulation via porous CaCO3 microparticles templating," Biomacromolecules **5**(5), 1962–1972 (2004).
64. E. W. Stein, D. V. Volodkin, M. J. McShane, and G. B. Sukhorukov, "Real-time assessment of spatial and temporal coupled catalysis within polyelectrolyte microcapsules containing coimmobilized glucose oxidase and peroxidase," Biomacromolecules **7**(3), 710–719 (2006).
65. J. Harris and S. Zalipsky, *Poly(Ethylene Glycol) Chemistry and Biological Applications*, Vol. 680 of ACS Symposium Series (American Chemical Society, 1997).
66. M. B. Mellott, K. Searcy, and M. V. Pishko, "Release of protein from highly cross-linked hydrogels of poly(ethylene glycol) diacrylate fabricated by UV polymerization," Biomaterials **22**(9), 929–941 (2001).
67. R. Russell, A. Axel, K. Shields, and M. Pishko, "Mass transfer in rapidly photopolymerized poly(ethylene glycol) hydrogels used for chemical sensing," Polymer (Guildf.) **42**(11), 4893–4901 (2001).
68. R. M. Rounds, B. L. Ibey, H. T. Beier, M. V. Pishko, and G. L. Coté, "Microporated PEG spheres for fluorescent analyte detection," J. Fluoresc. **17**(1), 57–63 (2006).
69. J. Lim, A. Chouai, S. T. Lo, W. Liu, X. Sun, and E. E. Simanek, "Design, synthesis, characterization, and biological evaluation of triazine dendrimers bearing paclitaxel using ester and ester/disulfide linkages," Bioconjug. Chem. **20**(11), 2154–2161 (2009).
70. Invitrogen, *Amine-Reactive Probes*, Aug. 17, 2010, http://probes.invitrogen.com/media/pis/mp00143.pdf.
71. E. Chang and D. Holguin, "Electrooptical light-management material: Low-refractive-index hydrogels," J. Adhes. **83**(1), 15–26 (2007).
72. W. M. Yunus and A. B. Rahman, "Refractive index of solutions at high concentrations," Appl. Opt. **27**(16), 3341–3343 (1988).
73. M. Mcshane and E. Stein, "Fluorescence-based glucose sensors," in *In Vivo Glucose Sensing*, D. D. Cunningham and J. A. Stenken , eds. (Wiley, (2010).
74. F. Hussain, D. J. Birch, and J. C. Pickup, "Glucose sensing based on the intrinsic fluorescence of sol-gel immobilized yeast hexokinase," Anal. Biochem. **339**(1), 137–143 (2005).

1. Introduction

Diabetes mellitus is a chronic disease where the body is unable to regulate its blood glucose concentration within normal physiological levels leading to secondary complications such as retinopathy, neuropathy, nephropathy, and cardiovascular disease [1,2] As of 2007, 17 million individuals in America lived with the disease, resulting in an economic burden totaling over 110 billion dollars in direct medical costs [3]. Proper management aims to improve diabetic outcomes by maintaining blood glucose levels within normal concentrations which typically includes an effective diet, exercise, and glucose monitoring program [1,4]. The effectiveness of diabetic management has been described by A1C values (glycated hemoglobin), an indicator of the mean glucose levels over several months [4,5]. While the most common method for monitoring blood glucose is the typical finger-stick approach [6], systems that allow for more-frequent sensing have been shown to be more effective in maintaining normal A1C values in adults. Therefore, the thrust of glucose sensing has been to develop a repeatable, long-lasting technique that can be used to maintain normal A1C levels while also increasing patient compliance. These A1C levels indicate the amount of hemoglobin that is glycated, which corresponds to the average glucose concentration in the plasma over several months [7].

The field of glucose-sensing as a whole has been widely explored and finely detailed by several groups [8–10]. Specifically, solutions based on the use of optical modalities for glucose sensing include Raman spectroscopy [11–14], optical coherence tomography (OCT) [15,16], photoacoustic spectroscopy [17–19], optical polarimetry [20–24], infrared spectroscopy [25,26], and fluorescence spectroscopy [27–32]. The optical technique being developed by our group has been a fluorescence intensity approach based on a competitive binding assay of fluorescently labeled Concanavalin A (Con-A) and a competing ligand that can function in the complex sample of interstitial fluid [33].

Con-A is a lectin that binds to carbohydrate moieties found in glycoproteins, glycolipids and various sugars in the presence of calcium and manganese divalent cations [34,35]. As reported previously, Con-A can exist as a tetramer and has been used as a component of glucose sensitive assays, specifically with dextran [28,36–38]. The biotoxicity of Con-A has been extensively studied, and has been shown to pose little to no adverse health risk in use for in vivo sensing at low concentrations [39]. In an attempt to decrease the irreversible binding

associated with the Con-A/dextran system, our group employed the use of glycosylated dendrimers as the competing ligand in a similar competitive assay [33]. Dendrimers are tree-shaped, globular macromolecules that have been explored for potential uses in chemotherapeutics [40,41], anti-viral pharmaceuticals [42–46], and scaffolds for tissue repair [47,48] due to their biocompatibility. Glycosylated dendrimers have also been used as a coating to significantly improve the biocompatibility of carbon nanotubes [49]. By adjusting the size and altering the functional end-groups of the dendrimers, the effective diameter, molecular weight, and hydrophilicity can be varied [50–52]. Using specifically tailored glycosylated dendrimers, our current assay employs the use of aggregation that is induced by competitive binding of multivalent components, which results in a fluorescence intensity that correlates to glucose concentration (Fig. 1). This combined assay and the protein individually have been shown to be functional for several days at body temperature (37 °C) [53].
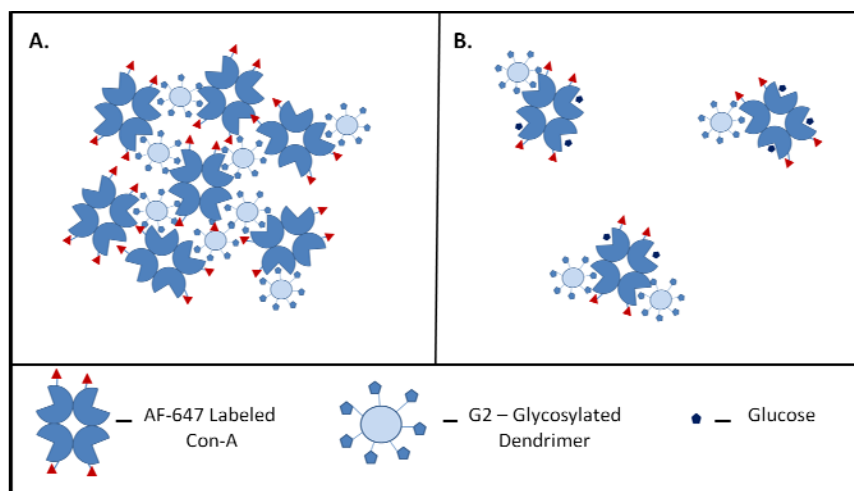

Fig. 1. This is a schematic representation of the aggregative nature used in the Con-A/dendrimer assay. With the assay exposed to low glucose concentrations (A) the assay emits lower fluorescence than when the assay is exposed to high glucose concentrations (B).

For functioning aggregative assays to be translated from the cuvette to implantable sensors, specifically tailored encapsulation methods which maintain the chemistry's binding kinetics must be employed. Requirements for such a strategy must include the withholding of components throughout the sensor's delivery and lifetime while allowing for the appropriate diffusion of the targeted analyte and subsequent response of the sensing chemistry. Much work in the field of encapsulation has been focused on the extension of drug delivery profiles. Concepts such as polymeric microspheres [54–56] and layer-by-layer (LbL) approaches [57–59] have been used and reported. These microencapsulation techniques have begun to be altered for general sensing purposes in attempt to meet the aforementioned requirements [60]. For example, several groups have loaded sacrificial spherical templates (i.e. melamine formaldehyde and calcium carbonate) with proteins and sensing chemistry that can then be exposed to alternating layers of poly-electrolytes which coat the template [61–63]. These cores can then be dissolved freeing the chemistry within the micron-sized LbL capsule that can then serve as a semi-permeable membrane for sensing purposes. Advantages of this technique include the fine level of control for the mesh size of the capsule and the high synthetic reproducibility. However, future work must be done to minimize the effects of electrostatic binding of the sensing chemistry to the charged interior wall of the capsule [64]. Additionally, groups have embedded sensing chemistries within a dense matrix in an attempt to maintain long-term functionality. Poly-(ethylene glycol) (PEG) has been employed in this manner due to its proven biocompatibility and hydrophilic nature [65]. Microspheres can be

created using PEG by crosslinking the individual chains via thermo-chemical or photo-chemical initiation, resulting in a mesh of PEG chains in which chemistry can be embedded. The effective pore size of this mesh can be altered by varying the average molecular weight of the PEG and/or changing the water content within the precursor solution prior to crosslinking [66,67]. With these variations, the mesh size for PEG can be tailored to be suitable for sensing purposes. However, the sensing response of assays embedded within this mesh has been limited in its reversibility due to the consistent mesh within these spheres without attachment of the assay to the polymeric backbone [68].

Until now, the successful encapsulation of the Con-A/glycodendrimer glucose sensing assay has not been reported. Previously, our group has proposed and presented an encapsulation strategy combining a water-in-oil emulsion technique with the addition of sugar crystals to the precursor PEG solution to form assay-filled pores within the hydrogel matrix of the microspheres. This microporation technique was shown to be functional with the Con-A/Dextran glucose sensitive assay – displaying a reversible response over several days [68]. Since microporated PEG spheres allowed competitive binding within the larger pores while providing for diffusion of smaller analytes due to the selectively permeable mesh, it was believed that similar biocompatible microporated microspheres may be candidates for housing the aggregative Con-A/glycodendrimer sensing assay. Work presented here explores the effectiveness of this technique in encapsulating the sensing chemistry with respect to its dynamic range, sensitivity, and reversibility.

2. Materials and methods

Concanavalin A (type IV), dimethyl sulfoxide (DMSO), trizma- hydrochloride (Tris-HCl), manganese chloride (MnCl2), sodium chloride (NaCl), D-glucose, D-mannitol, poly(ethylene glycol) diacrylate (PEG-DA) (Mn ~575), and light mineral oil were purchased from Sigma-Aldrich (St. Louis, MO). In addition, 1 M hydrochloric acid (HCl), 1 M sodium hydroxide (NaOH), and 0.1 M phosphate buffered saline (PBS) was purchased from Sigma-Aldrich. Alexa Fluor 647 - succinymidyl ester was purchased from Invitrogen (Carlsbad, CA), and sodium bicarbonate (NaHCO3) and dextrose were purchased from Fisher Scientific (Waltham, MA). Calcium chloride (CaCl2) was purchased from EMD Chemicals (Gibbstown, NJ). Sephadex beads (G75) were purchased from Amersham Biosciences (Waukesha, WI), and Darocur 1173 was purchased from CIBA Specialty Chemicals (Tarrytown, NY). Distilled water used in experiments was collected from the Millipore filtration system at 18 MΩ (Billerica, MA). Glycosylated dendrimers averaging 12 glucose moieties and 12 amine functional groups were received from Dr. Simanek's lab group at Texas A&M University using similar triazine architecture as that previously described [69]. Tris buffer used in these experiments was created via the formulation of 0.15 M NaCl, 0.1 M Tris-HCl, 1 mM CaCl2, and 1 mM MnCl2, and titrated with the appropriate aliquots of 0.1 M NaOH & 0.1 M HCl to adjust the pH to 7.3.

2.1. Labeling Concanavalin A

Con-A, the glucose receptor for the competitive binding assay, was labeled using the Amine-Reactive Protocol via Invitrogen. Briefly, 10 mg of Con-A was dissolved in 1 mL of 0.1 M sodium bicarbonate buffer (pH ~8.3) and 1 mg of Alexa Fluor 647 succinymidyl ester was added to 100 μL DMSO. The dye/DMSO was then added to the protein solution while it was being stirred, and the resultant was continuously stirred for one hour at room temperature to complete the reaction [70]. As approximately 1/4th of the dye actually binds to the amine groups on the Con-A tetramers, separation was performed on a Sephadex column made of G75 beads that had been swelled in TRIS buffer. Inactive Con-A and free dye were collected while passing TRIS buffer, and active labeled Con-A was eluted by passing a 200 mg/mL glucose solution through the column. This final collection volume was dialyzed against TRIS buffer with several buffer exchanges over the course of several days to remove the glucose

solution. This dialyzed fraction was concentrated by centrifugation, and the concentrations/labeling ratios were then determined by measuring the absorption spectra of the volumes. These measurements were performed by UV-VIS spectrometry indicating a labeling ratio of 4.7 dye molecules per Con-A tetramer. This solution was then diluted to 1.0 mg/mL with the addition of TRIS buffer.

2.2. Microsphere synthesis

Two groups of microspheres, hereafter called microporated-PEG and PEG-50, were created to display the functionality of the microporated microspheres. PEG-50 spheres are created with 50% water and 50% PEG, and microporated microspheres are created with pores within a 100% PEG solution. For comparison, schematic renditions of these are displayed in Fig. 2 as well as that of 100% PEG solution. PEG-50 spheres have shown to be effective in allowing the assay to respond with limited reversibility while PEG-100 spheres have been shown to have limited response but high reversibility [60]. Therefore, the microporation technique aims to capture the advantages of both by creating larger assay-filled pores within the tighter mesh of the PEG-100 spheres.

To create the porogen for the microporated PEG microspheres, 200 μL of AF-647 Con-A stock solution, 100 μL of G2-Dendrimer stock solution, 300 μL of PBS, and 20 mg of mannitol were added together. This precursor solution was mixed well, and then lyophilized overnight. In order to make the precursor polymeric solution for the microporation technique, 10 mg of the lyophilized sample was added to 1 mL PEG-DA (MW 575) and 10 μL Darocur. This solution was stirred to break up the lyophilized crystals into smaller particles. To make the polymeric precursor for the PEG-50 microspheres, 500 μL PEG-DA (MW 575), 100 μL ConA, 50 μL G2 Dendrimer, 350 μL TRIS buffer, and 10 μL Darocur were added together and mixed well.

A water-in-oil emulsion technique was implemented by adding 50 mL of light mineral oil to a 100 mL beaker. This solution was stirred via a magnetic stir plate, rotating at approximately 500 rpm. Under these conditions, the polymeric precursor was pipette into the beaker and allowed to spin for 15 seconds to create a fairly homogenous set of spheres. An ultraviolet light source (EFOS Ultracure 100SS Plus) at a wavelength of 365 nm was shone incident upon the beaker from a probe at 20 W/cm2 for 2.5 seconds to sufficiently cause the cross-linking via free-radical photo-initiation. Spheres were removed from the oil bath and vigorously rinsed with TRIS buffer via several buffer exchanges, and then added to a final solution of TRIS buffer. Spheres were stored at 4°C after synthesis.
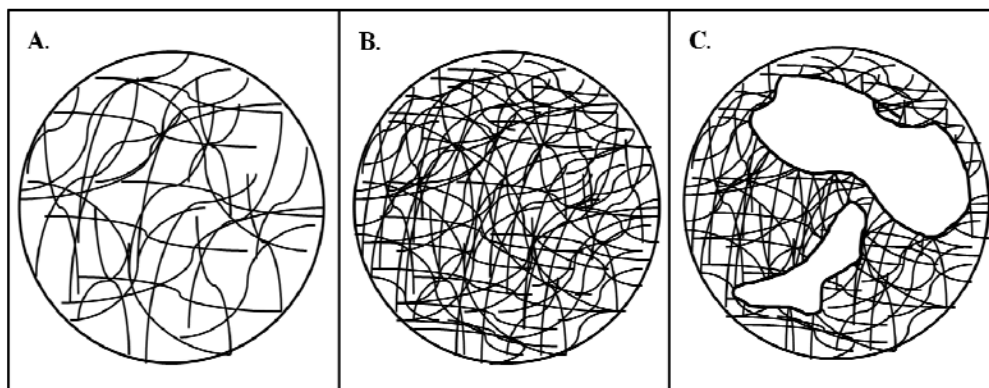

Fig. 2. This represents the mesh/pore sizes associated with various synthesized spheres. A represents PEG50 spheres (50% water, 50% PEG precursor) and has a very loose mesh. B represents PEG100 spheres (100% PEG precursor) and has a tight mesh. C represents microporated spheres (100% PEG with mannitol) that have large pores within the tighter mesh seen in B. These pores allow the sensing aggregation previously described.

2.3. Imaging spheres

To examine the average size of these particles, a bright-field microscopy technique was performed using a Leica DMLM microscope by adding a small volume of spheres on the surface of a microscope slide. To calculate the average diameter for each group of microspheres, ten images were captured by randomly translating the x-y motorized stage and focusing on the spheres within the image plane via a 10x objective. The diameters were calculated for each in-focus sphere that was taken, and the average diameter and standard deviation for each set was found.

The poration within the PEG microspheres was examined through the use of a confocal fluorescence microscope by taking slices of the collected fluorescence through the depth of the sphere. This was performed using a Leica TCS SP5 Confocal Microscope. For these experiments, a HeNe 632.8 nm laser was used at 4.5 mW with a 73.7 um pinhole and a 10x, 0.3 NA, dry objective. Images were taken without averaging and the resulting Z-step size was 2.383 μm with a 512 x 512 pixel resolution for the frame. This procedure was performed for both groups of the synthesized microspheres. Since these microspheres were comprised of a hydrogel material that largely consists of water, the refractive index of these spheres was approximately 1.37 [71]. These spheres were immersed in TRIS buffer (n = 1.33) for confocal scans. Therefore, the shape of the sphere did not display a significant distortion of the image as the index was somewhat matched.

2.4. Optical set up & fluorescent response to glucose

Fluorescent measurements with regards to leaching were performed on a commercially available spectrofluorometer system (Make: Photon Technology International, Model: Model L-201M Source, MP-1 Sample Compartment, and Model 814 Analog/Photon-Counting Photomultiplier Detector). In emission scan mode, the incident light was set to 633 nm and the emission monochromator was scanned from 650 nm to 710 nm with 1 nm steps and 1 second integration times. Fluorescent measurements of the sensing spheres with regard to response and long-term reversibility were taken with a custom-designed 90 degree fluorescence optical set up, represented in Fig. 3. A cuvette holder held the micro-cuvette containing the sensing spheres, and a 5 mW, HeNe 632.8 nm laser was made incident normal to its face. Due to the slight mismatch of refractive index between the spheres (1.37) and the buffer (1.33), there were multiple scattering events. Given the 1 cm pathlength of the cuvette, a 1 mm beam width, and scatter due to the packed spheres, the sampling volume is approximately 25 uL. This corresponded to approximately 250 spheres within that sampling volume. At 90 degrees,
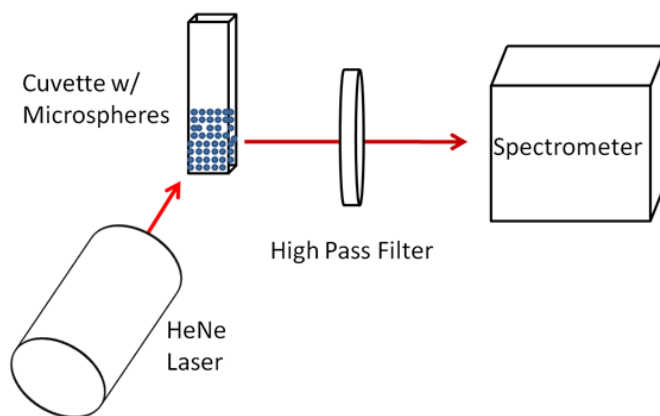

Fig. 3. This is a representation of the optical set up for 90-degree fluorescence measurements of sensing microspheres with a CCD Spectrometer and a HeNe 632.8 laser.

a Roper Scientific SpectraPro 150 spectrometer was placed with a fixed slit width, and a 650 nm long-pass, emission filter was used to eliminate stray laser light. The integration time of the system was 500 milliseconds to avoid saturation of the signal, and the grating had a blaze wavelength at 750 nm with 1200 grooves/mm. For collection purposes, the spectrometer was centered at 690 nm, collecting counts from 647 nm to 727 nm. This was performed to further minimize saturating the detector with scattered light from the source and in order to sufficiently measure the peak of the Alexa Fluor 647 emission at approximately 670 nm. The fluorescent intensity value used in all subsequent data analysis was the maximum value of the fluorophore emission for each spectrum collected.

2.5. Titration

For titration measurements, 500 μL of microporated microspheres were packed within a microcuvette and 2 mL of TRIS buffer were added. These microcuvettes were used to minimize the amount of spheres used. Highly concentrated, low volume aliquots of glucose were then added to the cuvette to make the surrounding solution increase in glucose concentration. This addition was performed without perturbing the settled spheres to assure adequate comparison. Sufficient time was given to allow for the diffusion of varying glucose concentrations into the spheres and for the response of the assay to achieve steady state. Three runs were performed for the microporated spheres and triplicate data was recorded for each run. The refractive index change between 0 mg/dL and 6000 mg/dL glucose levels have been shown to increase from 1.333 to 1.34 [72]. As the physiological glucose concentration are an order of magnitude less than this step change, the change in refractive index should be negligible when compared to the fluorescent response from the competitive binding chemistry.

In addition, the titration was performed on free assay in solution. A sensing assay was formulated in an attempt to mimic those concentrations and ratios seen within the microporated spheres for proper comparison. Specifically, 2 mL of TRIS buffer and 100 μL of 1 mg/mL Con-A was added to the cuvette. 50 μL of glycodendrimer was then added and given 1 hour to equilibrate and fluorescent measurements were taken resulting in an assay with 450 nM Con-A & 2.3 uM dendrimer. Aliquots of glucose were added to the system making glucose concentrations in step-wise fashion up to 1000 mg/dL. Steady state measurements were taken upon each addition after giving time for the system to equilibrate. Three runs were performed for the titration in free solution and triplicate data was recorded for each run.

2.6. Leaching

For the leaching experiments, 500 μL of both groups of microspheres that had not been exposed to glucose were packed in microcuvettes with the addition of 2 mL of TRIS buffer and given time to settle. Triplicate fluorescence spectra were then taken for baseline, 0 mg/dL glucose, measurements. Equivalent dilution factors were performed on each cuvette by adding 60 uL aliquots of 200 mg/mL glucose solutions to the settled spheres without perturbation to achieve glucose saturated solutions (600 mg/dL). To allow for the maximum response and any subsequent leaching, the spheres were given twenty-four hours upon the addition of glucose prior to triplicate fluorescence spectra being taken. Supernatant was then collected from the microcuvette and triplicate fluorescent spectra were taken to quantify the amount of leaching, if any, of the fluorescently labeled Con-A from within the microspheres.

2.7. Reversibility

The reversibility of the system was tested by packing 500 μL of microporated-PEG into a microcuvette and adding 2 mL of TRIS buffer. These spheres were allowed to settle, and triplicate baseline fluorescent readings were taken for each. A highly concentrated aliquot of glucose was then added to make the resulting solution 300 mg/dL. Fluorescent readings were

taken again six hours after the glucose was added to the cuvette to be assured the system was at steady-state. The remaining buffer in the microcuvette was then exchanged 4 times that evening, and exchanged 3 times the following morning to assure that the glucose concentration was effectively zero. This entire process was repeated for fourteen consecutive days.

3. Results & discussion

3.1. Bright field microscopy examples & size

Per the technique previously described, the average diameter of the microporated spheres was determined to be 545 μm with a standard deviation of 242 um. In comparison, the average diameter of the PEG-50 spheres was determined to be 476 um with a standard deviation of 174 um. As the ultimate application for these spheres is to be minimally invasive subcutaneous interstitial glucose sensors, they must be capable of being embedded interstitially. Therefore, future work will focus on reducing the average diameter by decreasing the size of the emulsified PEG droplets. However, for comparison purposes in this study the two sets of spheres were roughly the same size on average.

3.2. Poration

The crux of this work depends on the ability for pockets to be created that allow the Con-A/glycodendrimer sensing assay to be held within a tight polymeric mesh but also allow for diffusion of the glucose analyte and room for the aggregative assay to respond to the glucose concentration. From the fluorescence confocal microscopy images, the differences between PEG-50 spheres and microporated spheres are visualized. With a step size in the Z direction of 2.383 microns, these images show a slice through the interior of the spheres which display the fluorescent Con-A particles. For the microporated microspheres, the fluorescence is localized within striated pockets which are the residual imprint of sugar crystals that had since been dissolved. The average volume fraction of these pores is approximately 1% when accounting for the v/v% ratio between mannitol within the PEG precursor. In comparison, there is no such localization for PEG-50 spheres (Fig. 4). PEG-50 spheres do show a relatively
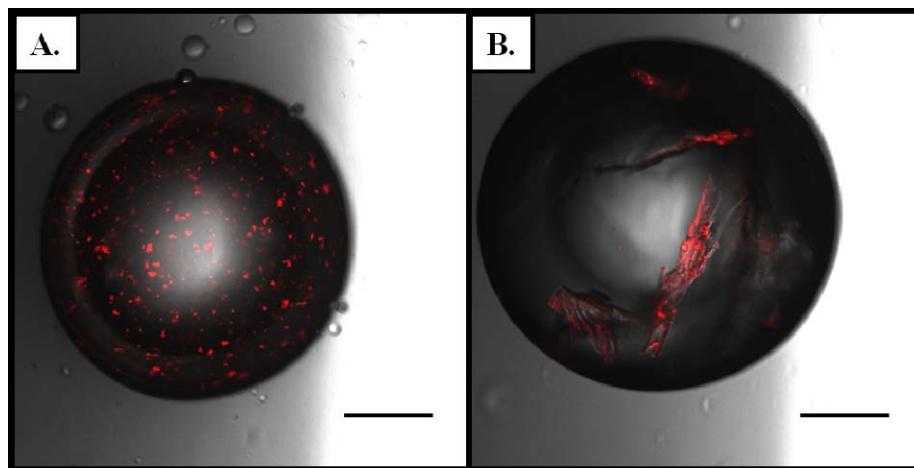

Fig. 4. These are hybrid images of false-colored confocal fluorescence slices overlaid onto bright-field images of the microspheres. The fluorescence displays the location of the labeled Con-A within the hydrogel, and it shows the differences of the pore distribution between PEG50 microspheres (A) and microporated microspheres (B). The large pores in B allow for the sensing mechanism to function effectively while maintaining reversibility by preventing leaching. The reference bar is 100 μm in length.

homogenous distribution of fluorescence; however, this distribution is a result of the non-localized withholding of sensing chemistry. Ultimately, it may be beneficial for the microporated microspheres to have a more homogenous distribution of size and distribution of pockets since a disperse population of sensing spheres with regard to these variables could result in a response that is dependent on which spheres are being interrogated. Future work will be done to minimize the variability by increasing the porogen to PEG ratio, increasing the speed of the homogenizer, adding surfactant to the precursor, and using a centrifugation/filtration system to retrieve the desired sphere-size.

3.3. Titration

Typically, the sensing response for an assay is inhibited by the specific attachment strategy due to the manipulation of the free binding kinetics. For an aggregative assay like the Con-A/glycodendrimer system described here, such strategies would result in prohibiting any response by preventing the mechanism, aggregation, to take place. Since this strategy does not purposely employ the use of a covalent/ionic attachment, and instead allows the chemistry to remain free within pores it was hoped that the sensing response would be present and similar to that seen in solution. Figure 5 displays the titration response to monotonic increasing concentrations of glucose for microporated microspheres. The microporated response is relatively linear from 50 to 200 mg/dL with a sensitivity of 1.3% per 10 mg/dL, and the response at 200 mg/dL is at 75% of the total response of the sensor. For comparison, Fig. 6 displays the fluorescent response for the sensing assay in solution across physiological concentrations of glucose as compared to the microporated response – displaying a linear response through 500 mg/dL of glucose and a sensitivity of 1.8% per 10 mg/dL. Above 500 mg/dL, the sensitivity decreases to approximately 0.4% per 10 mg/dL. In free solution, the sensing chemistry is at approximately 35% of the linear dynamic response at 200 mg/dL. The microporated sensing spheres do show a slightly greater sensitivity through the hypoglycemic range (0-100 mg/dL); however, there is an overall decrease in the dynamic range and
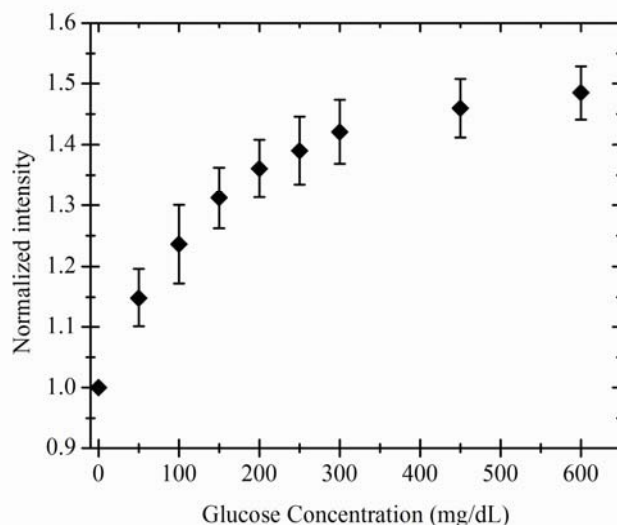

Fig. 5. Titration response to glucose: Glucose was titrated into a cuvette containing microporated microspheres. The system was given time to be at steady-state prior to readings. The intensity of the fluorescence is compared to the initial fluorescence seen at 0 mg/dL glucose concentration. Error bars depict the standard deviation through three separate titration runs.

fluorescent signal. A possible explanation for this decrease includes the variable loading of sensing components since the ratio of free/bound competing ligand is dependent on the concentration of the receptor and competing ligand for steady-state glucose concentrations. Therefore, any change in either the Con-A or glycodendrimer concentration within the pores will shift the response in a manner similar to that observed. This shift can also be attributed to the confinement of the aggregative sensing assay within pores, a process that can theoretically shift the distribution of aggregates to favor smaller particles in comparison to free solution with a given glucose concentration because of entropy requirements and steric hindrances presented by the pores. As the fluorescent response is dependent on the extent of competitive binding, this shift in aggregation can shift the response to mimic that seen at higher glucose concentrations of the assay in free solution.

The standard deviation seen in the titration response of the microporated spheres was also higher than that for the free assay. This can be attributed to the variation which was seen in the poration of the spheres. The rinsing of spheres required to eliminate the glucose within the buffer between runs may have resulted in a different subset of spheres being interrogated each time that ultimately could add noise to the system. As previously mentioned, the dynamic range of the assay is a function of the aggregation associated with competitive binding between the Con-A and glycosylated dendrimer. Therefore, the fluorescent response it is primarily dependent on the equilibrated glucose concentration. However, since the sensing chemistry is aggregative is nature, the dynamic range would be dependent on the size of the pores that contain the assay if they limited the extent of aggregation. The dynamic range of the sphere size should be independent of the individual sphere size and porosity, given that they allow for the appropriate size for individual pores.

The response time of the sensing chemistry within the spheres is primarily dependent on the diffusivity of hydrogel, the size of the spheres, and the porosity (volume fraction) of the spheres for whatever system they are placed in. Specifically, higher diffusivities should decrease response time for equilibrium, larger spheres should increase diffusion distances and increase response time, and higher porosity should decrease diffusion distances and decrease response time.
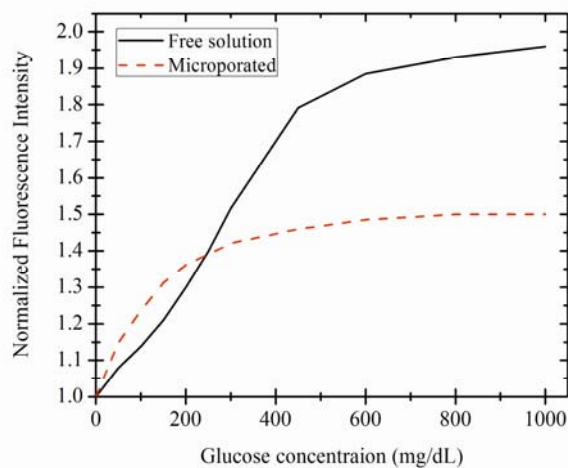

Fig. 6. Comparison of Response: This is the normalized fluorescent response of the assay in free solution compared to the normalized fluorescent response of the assay within microporated microspheres.

3.4. Leaching

The quantification of the leaching from within the microporated microspheres and PEG-50 microspheres is displayed by Fig. 7. Upon 24 hours of exposure to highly concentrated volumes of glucose (600 mg/dL), the supernatant showed insignificant values of fluorescence from the fluorescently labeled Con-A for microporated microspheres indicating that no leaching had occurred. In comparison, the plot of the fluorescence from the supernatant for the PEG-50 microspheres shows approximately 20% of the original fluorescence signal from the fluorescently labeled Con-A and confirms the problematic leaching associated with the PEG-50 polymeric mesh for encapsulation purposes. For these PEG-50 microspheres, the aggregates are sufficiently large to remain entrapped within the polymeric crosslinks at low concentrations of glucose. However, upon the addition of glucose, Con A competitively binds to the analyte rather than the glycodendrimer – decreasing the size of the aggregates. The fluorescently labeled Con-A chemistry attached to the glucose as well as the free glycosylated dendrimer is then capable of diffusing outwardly, into the supernatant. In contrast, the 100% PEG around the pores of the microporated microspheres seen via confocal microscopy is capable of withholding the assay throughout physiological concentrations of glucose due to the tighter mesh. As previously described, the long-term application of any sensing scheme requires an effective encapsulation/attachment method which disallows the undesirable release of key chemistry components. This leaching is effectively eliminated via the microporation technique and provides long-term functionality for the aggregative assay.
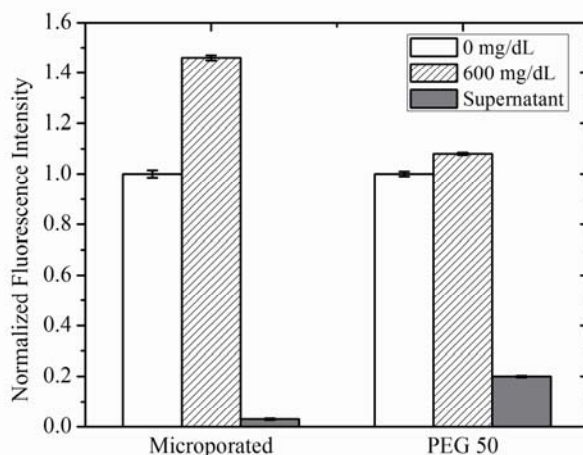

Fig. 7. Leaching Studies: Steady state fluorescent scans were taken for microporated and PEG50 microspheres at 0 mg/dL and 600 mg/dL. The supernatant was removed and scanned to determine if labeled Con-A leached out of the matrix. Fluorescence data is plotted relative to the initial 0 mg/dL scan. Error bars depict the standard deviation of the recorded measurements.

3.5. Reversibility

Fluorescent opto-chemical sensors often lose their functionality as a result of irreversible binding of the sensing components, photobleaching of the fluorophore, leaching of the chemistry, and/or the denaturing of the tertiary structure for the binding receptor [73,74]. In an attempt to address part of this potential problem with reversibility, glycosylated dendrimer was used in this system to avoid the increased binding affinity from a tetrameric unit of Con-A binding to multiple sites, such as what may occur for a long chain like dextran, and by using Alexa Fluor 647 which is more resistant than other fluorophores, such as the rhodamine

dyes, to photobleaching. As displayed in Fig. 8, the microporated microsphere sensor is shown to respond to cycling from 0 to 300 mg/dL glucose concentration over a duration of fourteen days. The key result is that there is reversibility with no drop off toward the end of the two weeks, a result that has not been previously displayed. In terms of absolute count, the signal from the microporated spheres show a declining trend as displayed in Fig. 8a. The majority of the aforementioned reasons for such a loss in functionality should be exponential in nature, but this absolute response does not appear to have a true exponential decay. This could be due to the combination of the effects on the aggregative assay. However, the relative increase from 0 mg/dL to 300 mg/dL each day shows no such trend as displayed in Fig. 8b. Therefore, a ratiometric sensing scheme using two fluorophores could be employed to maintain long-term functionality and reversibility. The relative results do show fluctuations in the response from day to day; however, as previously mentioned, we believe the variability in the relative readings between days is a result of polydispersity of the spheres in both the size and poration. Nonetheless, the data convincingly shows that microporated microspheres can effectively allow the sensing assay to remain functional and reversible to varying glucose concentrations through fourteen days at ambient conditions.
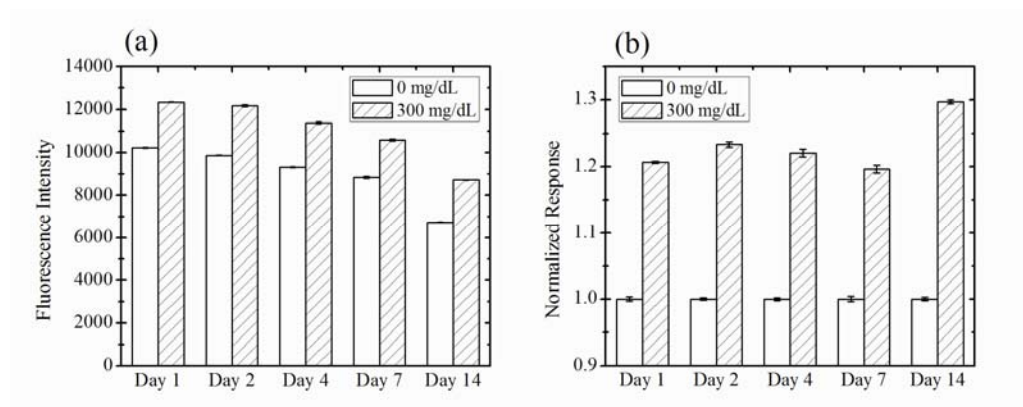

Fig. 8. Reversibility: Steady state fluorescent scans were taken each day at 0 mg/dL and 300 mg/dL glucose concentrations for a set of microporated microspheres. The absolute normalized fluorescent counts (a) and the relative daily increase fluorescence (b) are plotted for 0 mg/dL and 300 mg/dL for important days. Note that while there is a monotonic decrease in the absolute fluorescent intensity seen in (a), the relative fluorescent response (b) remains stable over this same time period. Error bars depict the standard deviation of the three recordings

4. Conclusion

In this work, the Con A/glycodendrimer glucose sensitive assay is shown, for the first time, to remain functional to varying glucose concentrations within polymeric microspheres. A microporation technique is used in which assay-filled pores are created within a polymeric mesh that allows the diffusion of glucose to the interior pockets while withholding the chemistry from outwardly diffusing throughout the competitive binding response. In addition, the microporation synthesis was shown to be advantageous for the aggregative sensing chemistry for several reasons: (1) it does not require the addition of powerful solvents to dissolve the porogen that could disrupt the tertiary structure of the protein, (2) the PEG hydrogel is hydrophilic and biocompatible which allows it to ultimately be implanted within the dermal layers of the tissue, and (3) the cross-linking between PEG chains is covalent which is not susceptible to electrostatic binding of the sensing chemistry to the inner surface. As a result, the sensing spheres were shown to be responsive to glucose with a sensitivity of 1.3% per 10 mg/dL glucose from 50 to 200 mg/dL. In addition, because of the tight mesh

surrounding the pores, there was shown to be effectively no leaching of the fluorescently labeled Con A from within the microporated microspheres.

Ultimately, for these microporated Con A/glycodendrimer sensing spheres to serve as ideal candidates for minimally invasive sensors for diabetics, in the future work several variables remain to be optimized, including; decreasing the response time by increasing the mesh size of the crosslinked PEG, making the pore-to-microsphere size ratio more homogeneous, and decreasing the overall size of the spheres.

Acknowledgments